Desalination and Water Treatment
www.deswater.com

doi: 10.5004/dwt.2021.27692

236 (2021) 240–249
October

CuO@MWCNTs nanocomposite as non-enzyme electrochemical sensor for the detection of Malathion in seawater

Eman Serag[a], Azza El-Maghraby[b], Nazly Hassan[c], Ahmed El Nemr[a,*]

[a]*Marine Pollution Department, Environmental Division, National Institute of Oceanography and Fisheries (NIOF), Kayet Bey, Elanfoushy, Alexandria, Egypt, emails: ahmedmoustafaelnemr@yahoo.com/ahmed.m.elnemr@gmail.com (A. El Nemr), d.emansearg@yahoo.com (E. Serag)*
[b]*Fabrication Technology Department, Advanced Technology and New Materials Institute, City of Scientific Research and Technological Applications (SRTA-City), Borg El-Arab, Alexandria, Egypt, email: maghrabyazza@yahoo.com*
[c]*Composite and Nanostructured Materials Department, Advanced Technology and New Materials Institute, City of Scientific Research and Technological Applications (SRTA-City), Borg El-Arab, Alexandria, Egypt, email: na_hassan12@yahoo.com*

Received 24 March 2021; Accepted 4 August 2021

ABSTRACT

This study used an enzyme-free electrochemical technique to identify low quantities of Malathion in sea water samples. The working electrode was made from carboxylated multiwall carbon nanotubes (c-MWCNTs) that were hybridised with copper oxide nanostructures (CuO NRs). Scanning electron microscopes (SEM) and transmission electron microscopes (TEM) were used to examine the morphology of the produced MWCNT and CuO NRs. X-ray diffraction was used to determine the crystallinity of produced materials. The electrochemical behavior of the non-enzymatic sensor was used to determine the presence of Malathion insecticides using linear sweep voltammetry (LSV), cyclic voltammetry (CV), and electrochemical impedance spectroscopy (EIS). Scanning electron microscopy and transmission electron microscope images showed that the produced MWCNT and CuO NRs were well-synthesized, and the CuO NRs were successfully connected to the growing MWCNT. The charge-transfer resistance (Ret) of the suggested c-MWCNT-CuO/GE and c-MWCNT-CuO/GE was lowered from 143 to 73.4Ω, showing improved electron transport and conductivity. The proposed c-MWCNT-CuO/GE had good electrochemical properties, such as a wide dynamic range (20–250 nM) and a low detection limit of 0.303 nM for the LSV approach. It had strong stability for 3 d, with a current response of 91 percent, high selectivity since the interference effect was less than 7%, and reproducibility was evaluated with five electrodes, yielding a standard deviation of 2.203%. The non-enzymatic sensor detected Malathion (organophosphorus insecticides) in aquatic environmental samples with recoveries ranging from 97% to 102% and relative standard deviations of less than 2%.

Keywords: Electrochemical sensor; Non-enzyme sensor; Malathion; CuO nanostructure; Carboxylated multiwall carbon nanotubes; Cyclic voltammetry

1. Introduction

Organic pesticides like organophosphorus pesticides (OPs) are commonly used to protect crops from pests [1]. They are, however, hazardous compounds and highly toxic substances that can harm both animals and humans [2–4]. They are absorbed in a variety of ways by the living body, many of which are severe [5–8]. Organochlorine pesticides are another type of organic chemical that is extremely dangerous to all living things. These herbicides pollute the environment and have serious environmental consequences [9–12]. Malathion (MLT) is a common OP with the chemical formula diethyl 2-[(dimethoxyphosphorothioyl)sulfanyl]

---

* Corresponding author.

This article was originally published with an error in the affiliations of Azza El-Maghrabhy and Nazly Hassan This version has been corrected. Please see Corrigendum in vol. 239 (2021) 301 [10.5004/dwt.2021.27999].

butanedioate. Excessive MLT use can be harmful to aquatic organisms, vertebrates, and humans by interfering with nervous systems, causing symptoms such as headaches and nausea, and suppressing the immune system at high doses. Furthermore, it pollutes groundwater and agricultural products [13,14]. As a result, detecting OPs requires a sensitive, precise, rapid, and dependable analytical approach. Gas chromatography with ECD and/or MS detectors [15–21], as well as liquid chromatography [22], have all been demonstrated to be extremely accurate and sensitive methods for detecting OPs. They do, however, face numerous challenges, such as large tools, high costs, and sophisticated operation and processing, all of which require time and effort. As a result, because of its simple operating procedures, low cost, quick turnaround time, and excellent repeatability and reproducibility, most modern research groups focus on the electrochemical approach [23].

Certain substances can be detected both enzymatically and non-enzymatically using the electrochemical approach [24–28]. The enzymatic electrochemical approach has some drawbacks, such as a time-consuming immobilisation procedure, high enzyme costs, and poor stability, repeatability, and reproducibility [29]. As a result, current research [23] is focusing on non-enzymatic electrochemical detection methods. Metal oxides such as CuO, ZnO, Fe_2O_3, Co_3O_4, and NiO have previously been used in non-enzymatic sensors [30,31].

CuO is a potent electrode material for non-enzymatic sensors when compared to other nanostructured transition metal oxides due to its natural availability, excellent electrocatalytic activity, low cost, relatively low resistance, and lower interference [32–34]. It also has a strong affinity for sulfur-containing compounds [35–37]. The detection technique is based on the detection of CuO's good redox peaks in a blank buffer system, which show significant suppression after the addition of Malathion to the solution, indicating an effect on CuO electrochemical behaviour.

CuO's poor conductivity, on the other hand, frequently influences current conduction rate, resulting in sensitivity reduction. CuO conductivity can be increased by changing the morphology and microstructure of the material, as well as by modifying the surface [38–40].

Carbon-based nanomaterials, particularly carbon nanotubes, have been shown to be suitable for sensor applications because they are conductive, easily functionalized, and have a large surface area. Carbon nanotubes (CNTs) are a type of nanomaterial with unique geometrical, mechanical, electrical, and chemical properties [41]. CNTs have excellent electrocatalytic activity and reduce surface fouling on electrochemical devices, making them ideal for electrochemical sensing. Carbon nanotube surfaces can be activated or functionalized. Molecules, enzymes, metal nanoparticles, and other molecules can be immobilised at oxygen-containing activated sites [42]. The number of studies that have developed non-enzymatic sensors using MWCNTs hybridised with polymer and metal nanoparticles has increased in recent years [43–49]. The hybridization process improves the functional qualities of each electrode component and harvests unique features through the interaction of electrode components [50,51].

Several carbon nanotube/CuO nanocomposites were used to detect organophosphate pesticides in the aquatic environment [52]. However, more research in this area is required before it can be used as a method of detecting contaminants. As a result, this study focuses on the non-enzymatic detection of MLT in seawater samples using a carboxylic multiwall carbon nanotube (c-MWCNT)/CuO nanostructure modified electrode. To characterise the fabricated materials, various approaches were used.

2. Materials and methods

2.1. Materials

Iron nitrate, cobalt nitrate hexahydrate, aluminum oxide, hydrazine hydrate ($N_2H_4{\cdot}5H_2O$, 80%), and ethylene glycol (EG, $C_2H_6O_2$, 99.5%), poly vinyl pyrrolidone (PVP) (MW = 40,000) ethanol (C_2H_5OH, 94%) were obtained from Sigma-Aldrich company and used directly without further purification. Copper sulfate pentahydrate, sodium hydroxide (NaOH, 98%), Nitric acid (HNO_3, 60%), and Sulfuric acid (H_2SO_4, 98%), were obtained from El-Nasr Co., Egypt. The supporting electrolyte, 0.1M phosphate–buffer solution (PBS) (pH 6) was prepared with sodium dihydrogen phosphate and sodium phosphate dibasic. All solutions were deoxygenated prior to each experiment using a flow of purified N_2 gas for 15 min. All chemical materials were used without further purification.

2.2. Instrument

The electrochemical measurements were measured via potentiostat (Gamary Instruments Electrochemical Analyzer, USA) in a three electrodes glass cell. Scanning electron microscope (SEM) images were obtained using JEOL Scanning Electron Microscope model JSM-6360LA, Japan and X-ray diffraction (XRD) analysis was conducted on Schimadzu-7000 X-Ray diffractometer using Cu Kα radiation with 1.5406 Å wavelength.

2.3. Methods

2.3.1. Synthesis of c-MWCNT

MWCNTs were grown on an iron–cobalt catalyst supported on aluminium oxide (Al_2O_3) in the presence of acetylene as a carbon source in previous work [53–55]. The reaction took place in a horizontal tube furnace with a flow rate of 70 mL/min of nitrogen gas and a flow rate of 30 mL/min of acetylene (C_2H_2) gas for 60 min.

The MWCNT was purified and functionalized with carboxylic groups using a 3:1 volume ratio of sulfuric acid (H_2SO_4) and nitric acid (HNO_3). The reaction mixture was sonicated for 30 min in an ultrasonic bath, then heated for 5 h at 70°C, diluted with deionized water, filtered, and washed with deionized water until it reached a neutral pH of 7. The carboxylic MWCNT (c-MWCNT) was dried in a vacuum oven at 70°C for 24 h.

2.3.2. Synthesis of copper oxide nanostructure (CuO NRs)

1.43 g of copper sulphate pentahydrate $CuSO_4{\cdot}5H_2O$, 2.4 g of sodium hydroxide NaOH, 0.8 g of poly vinyl pyrrolidone PVP, and 80 mL of ethylene glycol EG were mixed in a round flask and stirred at 120°C before adding 4.9 mL of hydrazine hydrate ($N_2H_4 \cdot 5H_2O$). The reaction was allowed to run for 90 min before being poured into deionized water containing 10% hydrazine hydrate and vigorously agitated to remove any remaining reactants and surfactants. The product was vacuum dried at 60°C for 24 h [56].

2.3.3. Manufacturing of carboxylic multiwall carbon nanotube – copper oxide (c-MWCNTs-CuO NRs) electrode

Preparation of carboxylic multiwall carbon nanotube-coper oxide hybridized as described in [52] with minor modifications. To obtain c-MWCNTs-CuO NRs suspension, copper oxide (CuO NRs) was suspended in 10 mg c-MWCNTs aqueous solution with a weight ratio of 2:1, and the mixture was sonicated for 30 min.

Prior to modification, the graphite electrode (GE) was polished with 0.05 µm aluminium oxide pastes to achieve a mirror-like shine. To remove inorganic impurities, the prepared electrode was immersed in deionized water and sonicated in an ultrasonic bath, followed by treatment with ethanol in an ultrasonic bath to remove organic impurities. To obtain c-MWCNTs-CuO/GE modified electrode, a 50 µL suspension of c-MWCNTs-CuO (NRs) was dropped on GE electrode using the casting method and allowed to dry under ambient air atmosphere. The control electrode modified with c-MWCNTs denoted as c-MWCNTs/GE. The c-MWCNTs-CuO/GE modified electrodes were then used as working electrode in the electrochemical cell with silver–silver chloride electrode (Ag/AgCl)) and graphite serving as reference and counter electrodes, respectively.

2.3.4. Electrochemical detection procedure

Electrochemical measurements were conducted in 0.1 M phosphate buffer PBS (pH 6.0). Cyclic voltammetry (CV) was performed at a potential from 0 to 0.4 V with the scan rate of 25 mV s^{-1}. Linear sweep voltammetry (LSV) was recorded via potential range from 1 to 0.4 V. Electrochemical impedance spectra (EIS) was carried out at a frequency ranging from 0.1 to 10,000 Hz. The Malathion detection was based on the relative current change ($\Delta I/I_0$) as the following formula.

$$\frac{\Delta I}{I_0}(\%) = \left[\frac{(I_0 - I)}{I_0}\right] \times 100 \qquad (1)$$

wherein I_0 and I are the anodic peak currents of the modified electrode treated without and with Malathion, respectively.

Fig. 1 depicts the fabrication scheme of the MWCNTs-CuO/GE sensor as well as the mechanism of electrochemical detection of Malathion. Malathion was absorbed on the electrode's surface, and its sulfur groups coordinated with the active site of CuO, obstructing the oxidation–reduction reaction of Cu^+ ions and decreasing the peak current [50,57].

2.3.5. Real sample analyses

To investigate whether the proposed electrode could be used to detect Malathion in seawater samples. The water was collected from the Elanfoushy area on Alexandria's Shores, filtered through a 0.45 µm membrane to remove all solid pollutants, and then spiked with varying amounts of Malathion. Finally, under ideal conditions, the fabricated c-MWCNTs-CuO/GE sensor was used to detect Malathion in various concentrations.

3. Results discussion

3.1. Characterization

The CVD-synthesized c-MWCNTs, as well as the synthesized CuO (NRs), are shown in SEM images in Fig. 2.

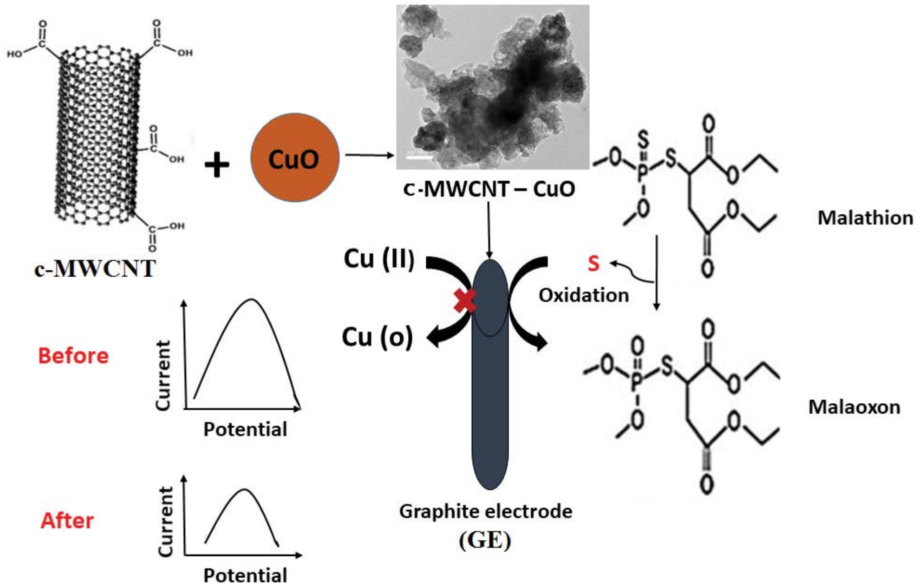

Fig. 1. Schematic illustration for the fabrication of c-MWCNTs-CuO/GE and the electrochemical detection of Malathion.

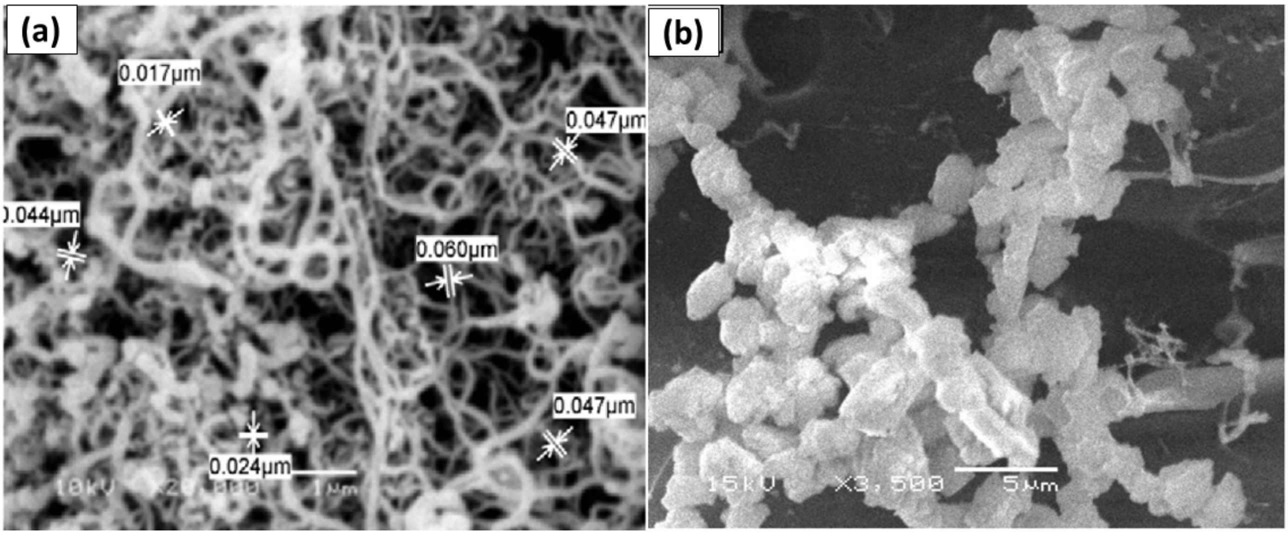

Fig. 2. SEM image of the synthesized: (a) MWCNT and (b) CuO NRs.

As demonstrated in Fig. 2a, the density c-MWCNTs are sufficiently entangled and free of amorphous carbon. In Fig. 2b, the synthesized CuO NRs are shown, which have a homogenous crystalline structure and a spherical shape with a higher tendency for agglomeration.

Another morphological investigation was carried out using transmission electron microscope analysis for the synthesized c-MWCNTs, CuO NRs, and c-MWCNT-CuO (NRs) nanocomposite, as shown in Fig. 3, which shows the smooth surface and low graphitization of the synthesized MWCNTs, as well as the circular shape of the synthesized CuO NRs. It also demonstrates that CuO was successfully attached to the surface of the c-MWCNT and that a full uniform layer of CuO was formed on the MWCNT surface.

XRD analysis of synthesized c-MWCNT, CuO NRs, and MWCNT-CuO hybrids are shown in Fig. 4. The c-MWCNT XRD pattern displays a significant peak at 2θ = 25.2° related to the hexagonal graphite structure. Due to an increase in the sp^2, C=C layers separation, this peak has shifted down from the peak of conventional graphite 2θ = 26.5° [51–53]. The prominent peaks in the CuO XRD pattern, on the other hand, show that the as-prepared CuO NRs have a monoclinic structure and good crystalline quality. The diffraction peaks at 2θ = 35.74°, 38.9°, 49.2°, and 74.1°, which correspond to (002), (111), (202), and (222), respectively, were in good agreement with standard ICDD Card No. 001-1117 and matched to previously reported ones [58,59]. The XRD pattern of MWCNT-CuO hybridised shows that all of the diffraction peaks assigned to MWCNT and CuO, and matched to the reported ones [60]. At 25.7°, the intense MWCNTs diffraction peak overlapped with that of CuO nanoparticles. The intensity of the other characteristic CuO peaks was lower. This reinforces the successful functionalization of MWCNTs with CuO nanoparticles [61].

The average crystallite size of the prepared CuO NRs and MWCNT-CuO hybridized were calculated via Scherer's formula as the following [60].

$$D = \frac{0.9\lambda}{\beta\cos\theta} \tag{2}$$

where k is a constant (about 0.9), λ is the X-ray wavelength (0.15418 nm), β is the full-width at half-maximum (FWHM) of the X-ray diffraction peak in radians and θ is the Bragg angle. Based on the Scherrer's equation, the average crystallite size for CuO and MWCNT-CuO hybridized were calculated and they were about 60.2 and 17.55 nm, respectively.

3.2. Electrochemical characterization of c-MWCNTs-CuO/GE

Fig. 5a shows cyclic-voltammetry (CV) of the modified electrodes c-MWCNTs/GE and c-MWCNTs-CuO/GE in KCl (0.1 M) containing $[Fe(CN)_6]^{3-/4-}$ (5 mM) at a scan rate 25 mV s^{-1}. Potassium chloride (KCl) is used as an electrolyte, which is an electrically conducting solution. Potassium ferrocyanide is a significant redox system that is chosen for its electrochemical reaction at the surface. Ferricyanide has a reversible one-electron redox performance for both c-MWCNTs-CuO/GE and c-MWCNTs/GE, as shown in Fig. 5a. The strong electro-catalytic activity and huge surface area of c-MWCNTs are responsible for the remarkable voltammetric response of the ferricyanide redox pair on the c-MWCNTs electrode. The current peak of the c-MWCNTs-CuO/GE electrode was higher than that of the c-MWCNTs/GE electrode, indicating that the CuO NRs have improved the electro-catalytic active surface area. The CV curve for the modified c-MWCNTs-CuO/GE in the absence and presence of 20 nM Malathion and 0.1 M phosphate buffer PBS (pH 6) is shown in Fig. 5b. The peak signals were further reduced after incubation of the modified electrode with Malathion, due to Malathion absorption on the surface of CuO, which resulted in the formation of a barrier that blocked the redox reaction of CuO NRs [14]. In 0.1 M PBS solution containing 20 nM Malathion, the effects of scan rate (10–90 mV s^{-1}) on the peak current of a c-MWCNT-CuO modified electrode are illustrated in Fig. 5c. With R^2 values of 0.986 and 0.984, the oxidation and reduction peaks increased linearly with the square root of the scan rate, indicating that the electrochemical reaction was a dielectric reaction [57].

To investigate the electron transfer rate at the electrode-electrolyte interface, electrochemical impedance

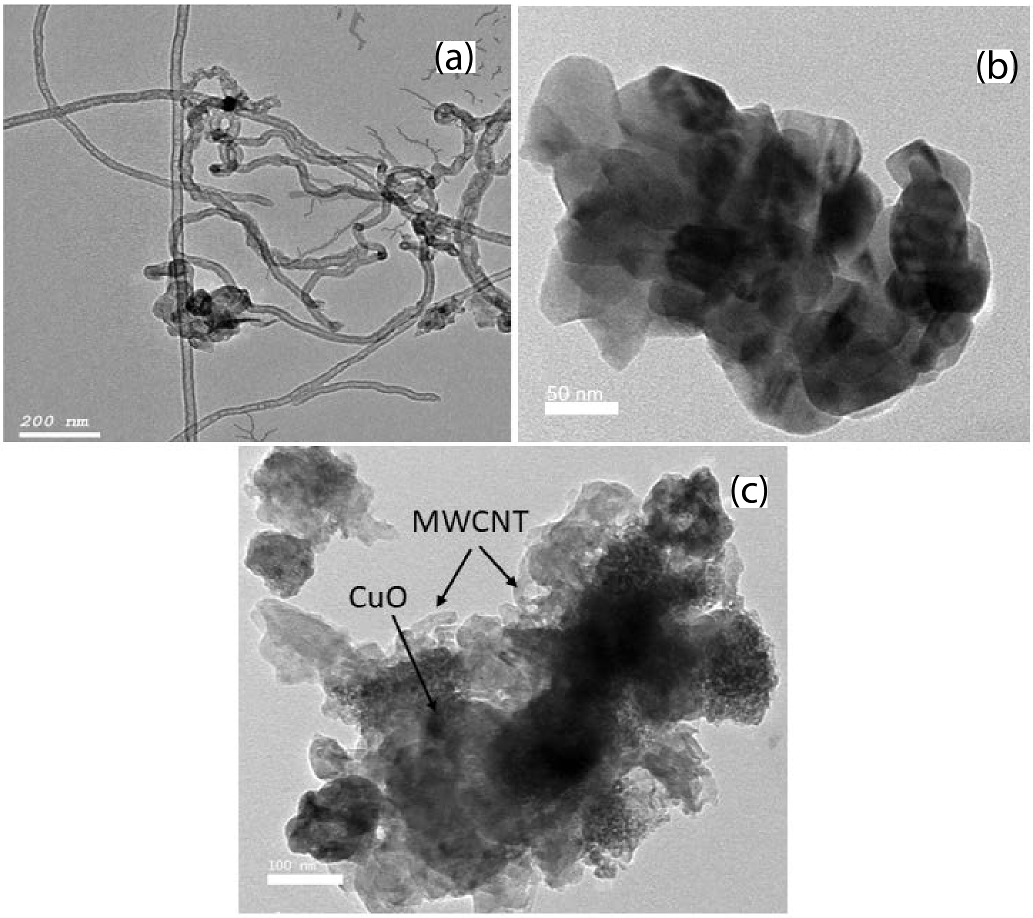

Fig. 3. TEM image of the synthesized: (a) c-MWCNT, (b) CuO NPs, and (c) c-MWCNT-CuO nanocomposite.

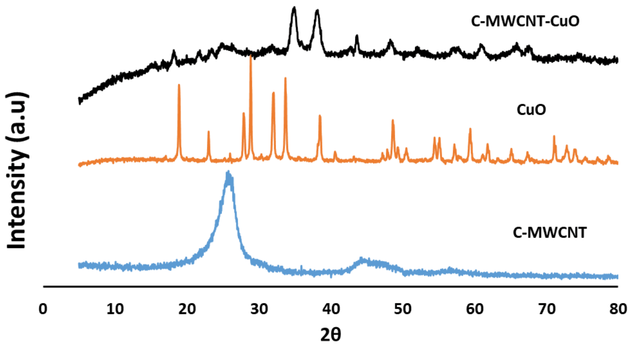

Fig. 4. XRD patterns for grown c-MWCNT, synthesized CuO NRs, and c-MWCNT-CuO hybridized.

spectroscopy (EIS) was used. At high frequencies, electron transfer is a limited process, with the charge-transfer resistance (Ret) equal to the semicircle part's diameter, whereas at low frequencies, electron transfer is accomplished through diffusion [54,55]. In the frequency range of 0.1 Hz to 100 kHz, the EIS of bare c-MWCNT/GE (a) and c-MWCNTs-CuO/GE (b) are given in Fig. 6. It can be shown that the Ret of c-MWCNT/GE is 143 Ω, while the Ret of c-MWCNTs-CuO/GE electrode is around 73.4 Ω, suggesting that the introduction of CuO NRs effectively enhances electron transfer and improves the conductivity.

3.3. Electrochemical detection of Malathion

LSV approach was employed to examine the efficiency of the Malathion detection at the c-MWCNTs-CuO/GE (Fig. 7). Different concentrations of Malathion were added to a PBS solution pH 6.0, and the current inhibition is proportional to the concentration of Malathion ranging from 20–250 nM. The linear curve fit a regression equation of $I = 17.29 + 0.0.05$ concentration with an R^2 of 0.983. The limit of detection (LOD) was calculated as three times the blank signal's standard deviation and was estimated to be 0.303 nM (S/N = 3). The linear range and detection limit of c-MWCNTs-CuO/GE were found to be quite similar to those of other Malathion non-enzymatic electrochemical sensors, as shown in Table 1.

3.4. Reproducibility and selectivity of the proposed sensor

The reproducibility of the modified electrodes c-MWCNTs-CuO/GE was tested by preparing five independent electrodes and measuring Malathion (20 nM) in

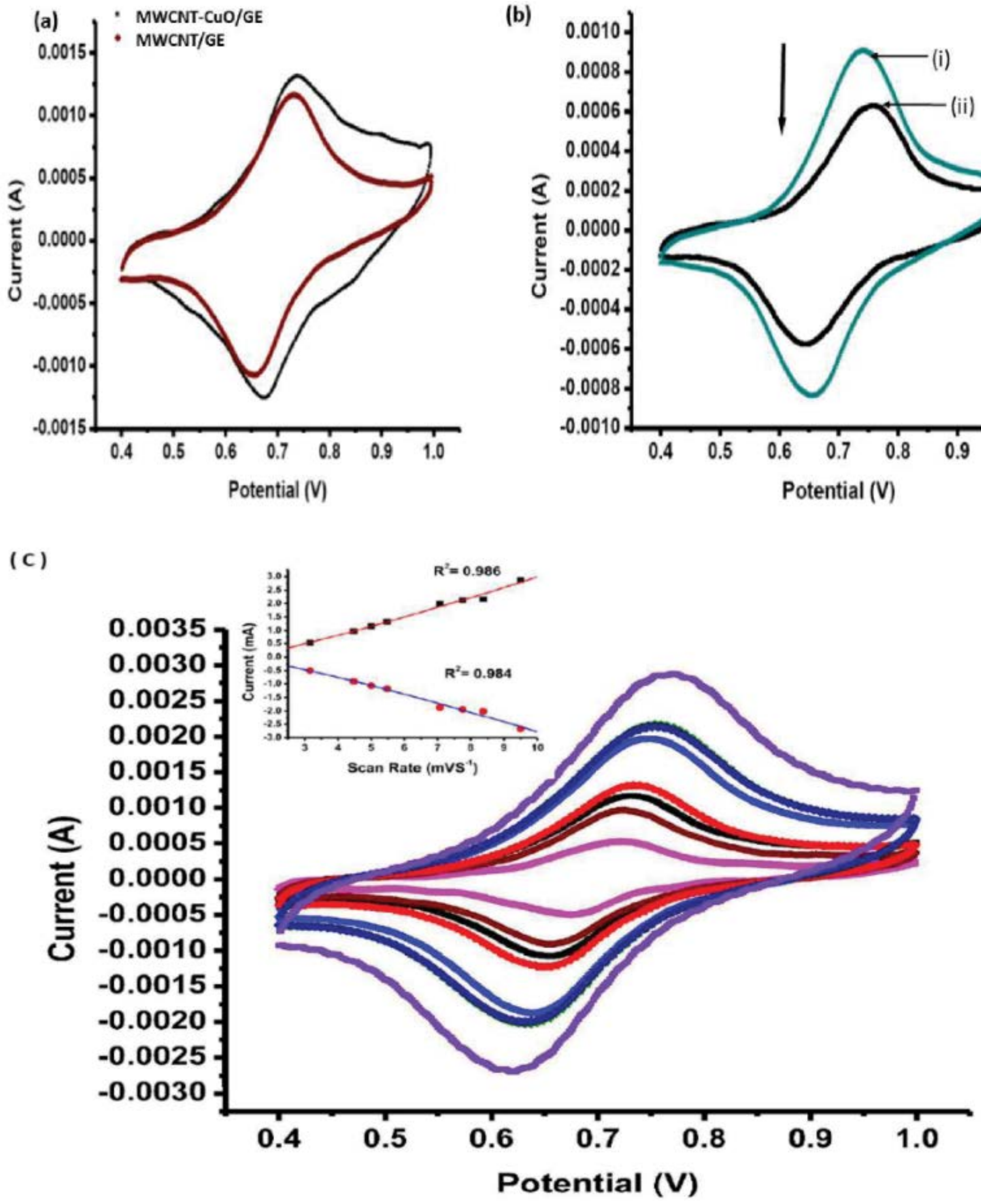

Fig. 5. (a) CV of c-MWCNTs/GE and c-MWCNTs-CuO/GE in 0.1 M KCl containing 5 mM $[Fe(CN)_6]^{3-/4-}$ at a scan rate 25 mV s^{-1}, (b) CV curve for (i) c-MWCNTs-CuO/GE in the absence and (ii) presence of 20 nM Malathion and 0.1 M PBS (pH 6), and (c) effects of scan rate (10–90 mV s^{-1}), the inset: plot of the current (mA) vs. the scan rate$^{1/2}$ (mV s^{-1})$^{1/2}$.

phosphate buffer pH 6 with an amperometric measurement. The relative standard deviation (RSD %) for three repeated experiments was 2.203%, demonstrating strong repeatability for c-MWCNTs-CuO/GE. The stability of the fabricated c-MWCNTs-CuO/GE electrode was tested using an amperometric signal sensing measurement of Malathion concentration (20 nM) every 3 d for three weeks. The current response in the test retained around 91% of the original measurement, showing that the manufactured electrode is stable. Malathion was detected electrochemically in the presence of interfering species such as common coexisting cations K^+, Na^+, anions such as Cl^-, SO_4^{-2}, and molecules such as glucose at concentrations 10-fold greater than Malathion (20 nM). In the presence of the inference, the signal change in Malathion detection was less than 7%, as shown in Fig. 8. The anti-interference ability of the fabricated electrode c-MWCNTs-CuO/GE can be attributed to the coordination between CuO NRs on the fabricated electrode and thiophosphoryl group of Malathion [49].

3.5. Detection of Malathion in real samples

The manufactured electrode c-MWCNTs-CuO/GE was utilized to detect Malathion in seawater samples to test the effectiveness of the proposed sensor. Malathion with known concentrations (20, 40, and 60 nM) was added after the pH was adjusted to 6.0 using 0.1 M phosphate buffer. Table 2 demonstrates that the suggested manufactured electrode functioned well in detecting Malathion in seawater, with recoveries ranging from 97 to 102% and RSDs of less than 2%.

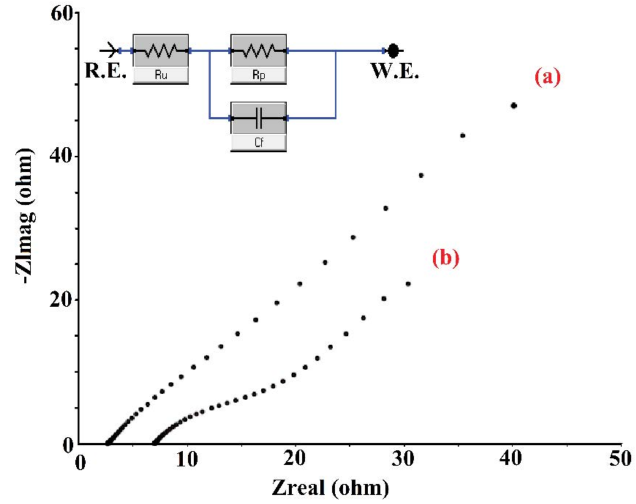

Fig. 6. Nyquist plots of (a) c-MWCNT/GE and (b) c-MWCNT-CuO/GE in 5 mM $[Fe(CN)_6]^{3-/4-}$ containing 0.1 M KCl at a frequency ranges of 0.1 Hz to 100 kHz, the inset represents the proposed equivalent circuit.

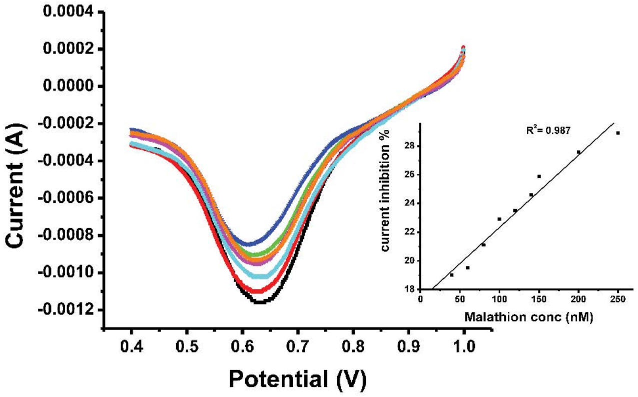

Fig. 7. LSV at a scan rate 10 mV s^{-1} responses of c-MWCNT-CuO/GE in PBS (pH 6.0) containing different concentrations of Malathion (20–250 nM), and LSV plots of the current inhibition % values against Malathion concentration.

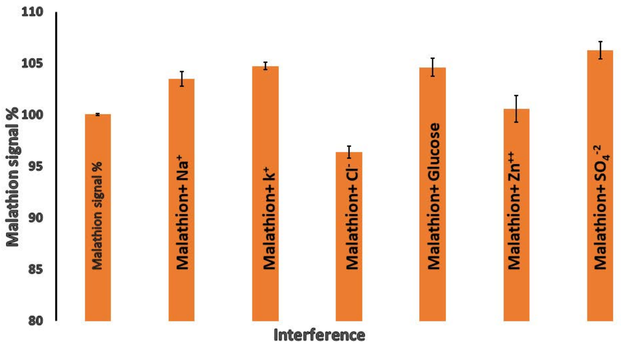

Fig. 8. The selectivity of the fabricated c-MWCNT-CuO/GE biosensors in 20 nM Malathion, with existing cations such as K^+, Na^+, and anions like Cl^-, SO_4^{2-}, and glucose with concentrations 10-fold higher than the concentration of Malathion.

Table 2
Detection of Malathion in real seawater samples using c-MWCNT-CuO/GE sensor

Sample	Added (nM)	Found (nM)*	Recovery (%)	RSD (%)
1	20	20.46	102.3	0.30
2	40	40.66	101.6	0.65
3	60	58.63	97.7	1.81

*Mean of three measurements.

Table 1
Comparison of different methods for Malathion detection

Modified electrode	Technique	Linear range (nM)	LOD (nM)	References
CuO-CMWCNT/GE	CV	20–300	0.143	This work
	LSV	20–250	0.303	This work
CuO-NPs/3DGR/GCE	DPV	0.03–1.5	0.01	[1]
CuO/SWCNT/GCE	DPV	0.3–1.4	0.3	[50]
PANI-ES/SWCNTs/CPE	DPV	200–1,400	200	[62]
Fe3O4NP/C-MWNT/Au	DPV	0.1–40	0.1	[63]
AuNP-CS-IL/PGE	SWV	0.89–5.94 and 5.94–44.6	0.68	[64]
Modified paper based electrodes	CV	20–60	20	[65]
PAn-PPy-MWCNTs	CV	0.03–75.0	0.003	[66]

4. Conclusion

Malathion was detected in an aquatic environment using the non-enzymatic electrochemical sensor c-MWCNTs-CuO/GE. The electrochemical activity of the manufactured c-MWCNTs-CuO/GE electrode was investigated using cyclic voltammetry and linear sweep voltammetry. Based on its suppressed signal measurement with a LOD of 0.303 within the concentration of Malathion of 20–250 nM using LSV, the established sensor demonstrated high sensitivity for Malathion detection. The established sensor also demonstrated high selectivity, long-term stability, and reproducibility. It was also effective at detecting Malathion in seawater samples, with a high percentage of recovery (97.0%–102.3%).

Author statement

Dr. Eman Serag conducted the experimental work of this article and contributed to the writing of this article. Professor Ahmed El Nemr supervised and provided financial support for this research and is the corresponding author of this article; Professor Azza El-Maghraby and Dr. Nazly Hassan collaborated on data analysis and discussion.

Acknowledgement

The corresponding author is grateful to the Science, Technology & Innovation Funding Authority (STDF) of Egypt for its partial financial support of this work (Project No. CB-4874).

References

[1] Y. Xie, Y. Yu, L. Lu, X. Ma, L. Gong, X. Huang, G. Liu, Y. Yu, CuO nanoparticles decorated 3D graphene nanocomposite as non-enzymatic electrochemical sensing platform for Malathion detection, J. Electroanal. Chem., 812 (2018) 82–89.

[2] A. El Nemr, Stereoselective Synthesis of Hydantocidin Analogues, J.L. Vicario, D. Badía, L. Carrillo, Eds., New Methods for the Asymmetric Synthesis of Nitrogen Heterocycles, Research Signpost, Transworld Research Network, Kerala, India, 2005, pp. 249–295.

[3] A. El Nemr, Ed., Impact, Monitoring and Management of Environmental Pollution, Nova Science Publishers, Inc., Hauppauge, New York, 2011.

[4] H.F. Asiri, A.M. Idris, T.O. Said, T. Sahlabji, M.M. Alghamdi, A.A. El-Zahhar, A. El Nemr, Monitoring and health risk assessment of some pesticides and organic pollutants in fruit and vegetables consumed in Asir Region, Saudi Arabia, Fresenius Environ. Bull., 29 (2020) 615–625.

[5] D. Guillén, A. Ginebreda, M. Farré, R.M. Darbra, M. Petrovic, M. Gros, D. Barceló, Prioritization of chemicals in the aquatic environment based on risk assessment: analytical, modeling and regulatory perspective, Sci. Total Environ., 440 (2012) 236–252.

[6] X. Wang, X. Lu, J. Chen, Development of biosensor technologies for analysis of environmental contaminants, Trends Environ. Anal. Chem., 2 (2014) 25–32.

[7] R. Ali, K. Richard, Z. Hussain, A. Tahira, S. Tufail, H. Sherazi, M. Willander, Amino acid assisted growth of CuO nanostructures and their potential application in electrochemical sensing of organophosphate pesticide, Electrochim. Acta, 190 (2016) 972–979.

[8] F.L. Migliorini, R.C. Sanfelice, L.A. Mercante, M.H.M. Facure, D.S. Correa, Electrochemical sensor based on polyamide 6/polypyrrole electrospun nanofibers coated with reduced graphene oxide for Malathion pesticide detection, Mater. Res. Express, 7 (2019) 015601.

[9] A. El Nemr, M.M. El-Sadaawy, Polychlorinated biphenyl and organochlorine pesticide residues in surface sediments from the Mediterranean Sea (Egypt), Int. J. Sediment Res., 31 (2016) 44–52.

[10] A. El Nemr, G.F. El-Said, A. Khaled, Risk assessment of organochlorines in mollusk from the Mediterranean and Red Sea of Coasts (Egypt), Water Environ. Res., 88 (2016) 325–337.

[11] S. Ragab, A. El Sikaily, A. El Nemr, Concentrations and sources of pesticides and PCBs in surficial sediments of the Red Sea Coast, Egypt. J. Aquat. Res., 42 (2016) 365–374.

[12] D.M.S.A. Salem, A. El Sikaily, A. El Nemr, Organochlorines and their risk in marine shellfish collected from the Mediterranean coast, Egypt, Egypt. J. Aquat. Res., 40 (2014) 93–101.

[13] N. Kaur, H. Thakur, N. Prabhakar, Multi walled carbon nanotubes embedded conducting polymer based electrochemical aptasensor for estimation of Malathion, Microchem. J., 147 (2019) 393–402.

[14] C.S. Kushwaha, S.K. Shukla, Non-enzymatic potentiometric Malathion sensing over chitosan-grafted polyaniline hybrid electrode, simultaneous determination of nine trace organophosphorous pesticide residues in fruit samples using molecularly imprinted matrix solid-phase dispersion followed by gas chromatography, J. Mater. Sci., 54 (2019) 10846–10855.

[15] X. Wang, X. Qiao, Y. Ma, T. Zhao, Z. Xu, J. Agric, Simultaneous determination of nine trace organophosphorous pesticide residues in fruit samples using molecularly imprinted matrix solid-phase dispersion followed by gas chromatography, Food Chem., 61 (2013) 3821–3827.

[16] H.F.M. Asiri, A.M. Idris, T.O. Said, T. Sahlabji, M.M. Alghamdi, A.A. El-Zahhar, A. El Nemr, Monitoring and health risk assessment of some pesticides and organic pollutants in fruit and vegetables consumed in Asir Region, Saudi Arabia, Fresenius Environ. Bull., 29 (2020) 615–625.

[17] D.M.S. Salem, A. Khaled, A. El Nemr, Assessment of pesticides and polychlorinated biphenyls (PCBs) in sediments of the Egyptian Mediterranean Coast, Egypt. J. Aquat. Res., 39 (2013) 141–152.

[18] A. El Nemr, Ed., Impact, Monitoring and Management of Environmental Pollution, Nova Science Publishers, Inc., Hauppauge, New York, 2011.

[19] A. El Nemr, Ed., Environmental Pollution and its relation to Climate Change, Nova Science Publishers, Inc., Hauppauge, New York, 2012.

[20] A. El Nemr, Ed., Pollution Status, Environmental Protection, and Renewable Energy production in Marine Systems, Nova Science Publishers, Inc., Hauppauge, New York, 2016.

[21] A. El Nemr, A.A. Moneer, A. Khaled, A. El-Sikaily, Levels, distribution and risk assessment of organochlorines in surficial sediments of the Red Sea Coast, Egypt, Environ. Monit. Assess., 185 (2013) 4835–4853.

[22] M.A. Farajzadeh, M. Bahram, M.R. Vardast, M. Bamorowat, Dispersive liquid–liquid microextraction for the analysis of three organophosphorus pesticides in real samples by high performance liquid chromatography-ultraviolet detection and its optimization by experimental design, Microchim. Acta, 172 (2010) 465–470.

[23] C. Yang, R. Devasenathipathy, K. Kohila Rani, S. Wang, synthesis of multiwall carbon nanotubes covered copper oxide nanobarrier for senstive and selective electrochemical determination of hydrogen peroxide, Int. J. Electrochem. Sci., 12 (2017) 5910–5920.

[24] A. Khan, A.A.P. Khan, A.M. Asiri, K.A. Alamry, Preparation and characterization of hybrid graphene oxide composite and its application in paracetamol microbiosensor, Polym. Compos., 30 (2015) 221–228.

[25] A. Khan, A.A.P. Khan, M.M. Rahman, A.M. Asiri, K.A. Alamry, Preparation of polyaniline grafted graphene oxide-WO_3 nanocomposite and its application as a chromium(III) chemisensor, RSC Adv., 5 (2015) 105169–105178.

[26] A. Khan, A.A. Parwaz Khan, A.M. Asiri, B.M. Abu-Zied, Green synthesis of thermally stable Ag-rGO-CNT nano composite with high sensing activity, Composites, Part B, 86 (2016) 27–35.

[27] A. Khan, A.A. Parwaz Khan, M.M. Rahman, A.M. Asiri, Inamuddin, K.A. Alamry, S.A. Hamed, Preparation and characterization of PANI@G/CWO nanocomposite for enhanced 2-nitrophenol sensing, Appl. Surf. Sci., 433 (2018) 696–704.

[28] A.A. Khan, U. Habiba, A. Khan, Synthesis and characterization of organic-inorganic nanocomposite poly-o-anisidine Sn(IV) arsenophosphate: its analytical applications as Pb(II)

ion-selective membrane electrode, Int. J. Anal. Chem., 2009 (2009) 659215, doi: 10.1155/2009/659215.

[29] D. Huo, Q. Li, Y. Zhang, C. Hou, Y. Lei, A highly efficient organophosphorus pesticides sensor based on CuO nanowires–SWCNTs hybrid nanocomposite, Sens. Actuators, B, 199 (2014) 410–417.

[30] Q. Dong, H. Ryu, Y. Lei, Metal oxide based non-enzymatic electrochemical sensors for glucose detection, Electrochim. Acta, 370 (2021) 137744, doi: 10.1016/j.electacta.2021.137744.

[31] X. Zhou, X. Gu, Z. Chen, Y. Wu, W. Xu, J. Bao, A novel and sensitive Cu_2ZnSnS_4 quantum dot–based non–enzymatic glucose sensor, Sens. Actuators, B, 329 (2021) 129117, doi: 10.1016/j.snb.2020.129117.

[32] I.U. Hassan, H. Salim, G.A. Naikoo, T. Awan, R.A. Dar, F. Arshad, M.A. Tabidi, R. Das, W. Ahmed, A.M. Asiri, A.H. Qurashi, A review on recent advances in hierarchically porous metal and metal oxide nanostructures as electrode materials for supercapacitors and non-enzymatic glucose sensors, J. Saudi Chem. Soc., 25 (2021) 101228, doi: 10.1016/j.jscs.2021.101228.

[33] P. Yang, X. Wang, C.Y. Ge, X. Fu, X.Y. Liu, H. Chai, K. Chen, Fabrication of CuO nanosheets-built microtubes via Kirkendall effect for non-enzymatic glucose sensor, Appl. Surf. Sci., 494 (2019) 484–491.

[34] M. Sabbaghan, A.S. Shahvelayati, K. Madankar, Synthesis and characterization of micro-mesoporous MCM-41 using various ionic liquids as co-templates, Spectrochim. Acta, Part A, 135 (2015) 662–668.

[35] J. Yang, W. Tan, C. Chen, Y. Tao, Y. Qin, Y. Kong, Nonenzymatic glucose sensing by CuO nanoparticles decorated nitrogen-doped graphene aerogel, Mater. Sci. Eng., C, 78 (2017) 210–217.

[36] D. Du, J. Ding, J. Cai, A. Zhang, One-step electrochemically deposited interface of chitosan–gold nanoparticles for acetylcholinesterase biosensor design, J. Electroanal. Chem., 605 (2007) 53–60.

[37] R.X. Zhang, P. Yang, Y.X. Zhang, A novel high-sensitivity non-enzymatic glucose sensor via $Cu_2O@CuO@NiCo_2O_4$ nanowires as catalyst, Mater. Lett., 272 (2020) 127850, doi: 10.1016/j.matlet.2020.127850.

[38] Y. Zheng, Z. Liu, Y. Jing, J. Li, H. Zhan, An acetylcholinesterase biosensor based on ionic liquid functionalized graphene–gelatin-modified electrode for sensitive detection of pesticides, Sens. Actuators, B, 210 (2015) 389–397.

[39] Y. Wang, S. Zhang, W. Bai, J. Zheng, Layer-by-layer assembly of copper nanoparticles and manganese dioxide-multiwalled carbon nanotubes film: a new nonenzymatic electrochemical sensor for glucose, Talanta, 149 (2016) 211–216.

[40] R.F. Gao, J.B. Zheng, Amine-terminated ionic liquid functionalized carbon nanotube-gold nano particles for investigating the direct electron transfer of glucose oxidase, Electrochem. Commun., 11 (2009) 608–611.

[41] R. Prasad, B.R. Bhat, Multi-wall carbon nanotube-NiO nanoparticle composite as enzyme-free electrochemical glucose sensor, Sens. Actuators, B, 220 (2015) 81–90.

[42] R. Sedghi, Z. Pezeshkian, Fabrication of non-enzymatic glucose sensor based on nanocomposite of MWCNTs-COOH-Poly(2-aminothiophenol)-Au NPs, Sens. Actuators, B, 219 (2015) 119–124.

[43] Y. Zhang, E. Zhou, Y. Li, X. He, A novel nonenzymatic glucose sensor based on magnetic copper ferrite immobilized on multiwalled carbon nanotubes, Anal. Methods, 7 (2015) 2360–2366.

[44] A.C. De Sá, A. Cipri, A. González-Calabuig, N.R. Stradiotto, M. Del Valle, Resolution of galactose, glucose, xylose and mannose in sugarcane bagasse employing a voltammetric electronic tongue formed by metals oxy-hydroxide/MWCNT modified electrodes, Sens. Actuators, B, 222 (2016) 645–653.

[45] K. Dhara, D.R. Mahapatra, Review on electrochemical sensing strategies for C-reactive protein and cardiac troponin I detection, Microchem. J., 156 (2020) 104857, doi: 10.1016/j.microc.2020.104857.

[46] C.-S. Liu, J. Li, H. Pang, Metal-organic framework-based materials as an emerging platform for advanced electrochemical sensing, Coord. Chem. Rev., 410 (2020) 213222, doi: 10.1016/j.ccr.2020.213222.

[47] A.S. Shamsabadi, H. Tavanai, M. Ranjbar, A. Farnood, M. Bazarganipour, Electrochemical non-enzymatic sensing of glucose by gold nanoparticles incorporated graphene nanofibers, Mater. Today Commun., 24 (2020) 100963, doi: 10.1016/j.mtcomm.2020.100963.

[48] R. Devasenathipathy, C. Karuppiah, S.M. Chen, S. Palanisamy, B.S. Lou, M.A. Ali, F.M.A. Al-Hemaid, A sensitive and selective enzyme-free amperometric glucose biosensor using a composite from multi-walled carbon nanotubes and cobalt phthalocyanine, RSC Adv., 5 (2015) 26762–26768.

[49] N. Anzar, R. Hasan, M. Tyagi, N. Yadav, J. Narang, Carbon nanotube – a review on synthesis, properties and plethora of applications in the field of biomedical science, Sens. Int., 1 (2020) 100003.

[50] D. Huo, Q. Li, Y. Zhang, C. Hou, Y. Lei, A highly efficient organophosphorus pesticides sensor based on CuO nanowires–SWCNTs hybrid nanocomposite, Sens. Actuators, B, 199 (2014) 410–417.

[51] E. Serag, A. El Nemr, F.F. Abdel Hamid, S.A. Fathy, A. El-Maghraby, A novel three dimensional carbon nanotube-polyethylene glycol – polyvinyl alcohol nanocomposite for Cu(II) removal from water,Egypt. J. Aquat. Biol. Fish., 22 (2018) 103–118.

[52] S.A. Fathy, F.F. Abdel Hamid, A. El Nemr, A. El-Maghraby, E. Serag, Novel tyrosinase biosensor based on multiwall carbon nanotube – titanium oxide nanocomposite for catechol determination, Desal. Water Treat., 130 (2018) 98–108.

[53] A. El Nemr, E. Serag, A. El-Maghraby, S.A. Fathy, F.F.A. Hamid, Manufacturing of pH sensitive PVA/PVP/MWCNT and PVA/PEG/MWCNT nanocomposites: an approach for significant drug release, J. Macromol. Sci. A, 56 (2019) 781–793.

[54] D. Park, H. Ju, T. Oh, J. Kim, A p-type multi-wall carbon nanotube/Te nanorod composite with enhanced thermoelectric performance, RSC Adv., 8 (2018) 8739–8746.

[55] J. Ding, H. Zhang, F. Jia, W. Qin, D. Du, Assembly of carbon nanotubes on a nanoporous gold electrode for acetylcholinesterase biosensor design, Sens. Actuators, B, 199 (2014) 284–290.

[56] B.J. Yuan, R. Zhang, H. Zhang, X. Shi, Y. Guo, X. Guo, S. Guo, D. Cai, Zhang, Electrochemical and electrocatalytic properties of a stable Cu-based metal–organic framework, Int. J. Electrochem. Sci., 10 (2015) 4899–4910.

[57] Y. Xie, Y. Yu, L. Lu, X. Ma, L. Gong, X. Huang, G. Liu, Y. Yu, CuO nanoparticles decorated 3D graphene nanocomposite as non-enzymatic electrochemical sensing platform for Malathion detection, J. Electroanal. Chem., 812 (2018) 82–89.

[58] K. YunKyoung, C. Seungil, L. JunHo, H. Soon, Aerosol approach for hollow spheres of a porous 3D carbon nanotube/CuO network and their anodic properties for lithium-ion battery, J. Nanosci. Nanotechnol., 14 (2014) 9143–9147.

[59] B. Shaswat, C. Pronobesh, P. Mayur, K. Bolin, K. Niranjan, Hyperbranched epoxy/MWCNT-CuO-nystatin nanocomposite as a high performance, biocompatible, antimicrobial material, Mater. Res. Express., 1 (2014) 045402.

[60] M.M. Hussain, A.M. Asiri, M.M. Rahman, A non-enzymatic electrochemical approach for L-lactic acid sensor development based on CuO·MWCNT nanocomposites modified with a Nafion matrix, New J. Chem., 44 (2020) 9775–9787.

[61] A. Rwaida, A. Nehad, A. Mai, S. Ebtesam, M. Shaza, F. Nida. Nanoparticles based solid contact potentiometric sensor for the determination of theophylline in different types of tea extract, Inorg. Chem. Commun., 119 (2020) 108080.

[62] A.M. Al'Abri, S.N. Abdul Halim, N.K. Abu Bakar, S.M. Saharin, B. Sherino, H. Rashidi Nodeh, S. Mohamad, Highly sensitive and selective determination of Malathion in vegetable extracts by an electrochemical sensor based on Cu-metal organic framework, Environ. Sci. Health B, 54 (2019) 930–941.

[63] N. Chauhan, C.S. Pundir, An amperometric biosensor based on acetylcholinesterase immobilized onto iron oxide nanoparticles/

multi-walled carbon nanotubes modified gold electrode for measurement of organophosphorus insecticides, Anal. Chim. Acta, 701 (2011) 66–74.

[64] G. Bolat, S. Abaci, Non-enzymatic electrochemical sensing of Malathion pesticide in tomato and apple samples based on gold nanoparticles-chitosan-ionic liquid hybrid nanocomposite, Sensors, 18 (2018) 773, doi: 10.3390/s18030773.

[65] T. Wang, R.C. Reid, S.D. Minteer, A paper-based mitochondrial electrochemical biosensor for pesticide detection, Electroanalysis, 28 (2016) 854–859.

[66] L. He, B. Cui, J. Liu, Y. Song, M. Wang, D. Peng, Z. Zhang, Novel electrochemical biosensor based on core-shell nanostructured composite of hollow carbon spheres and polyaniline for sensitively detecting Malathion, Sens. Actuators, B, 258 (2018) 813–821.